P-156: Electrically Stabilized Four-Domain Twisted Nematic Structure with High Transmittance and Fast Response

Jin-Hee Jeong[1], Tae-Min Kim[2], Min-Geon Choi[2], Yeon-Kyu Moon[2], You-Jin Lee[1], Jae-Hoon Kim[1,2], and Chang-Jae Yu[1,2]

[1]Department of Electronic Engineering, Hanyang University, Seoul 133-791, Korea
[2]Department of Information Display Engineering, Hayang University, Seoul 133-791, Korea

Abstract

We propose a novel method for a stable four-domain twisted nematic (4DTN) structure by injecting nematic liquid crystal in an isotropic phase under an applied electric field. In this method, no high pre-tilt angle is required to stabilize the 4DTN structure and thus the high transmittance and fast response are obtained.

1. Introduction

The twisted nematic (TN) liquid crystal display (LCD) mode has been widely used in various display applications due to its simple manufacturing process and high light efficiency. However, TN mode hardly used in the large size displays such as television sets due to its poor viewing angle characteristics and gray inversion problem [1]. To improve the viewing angle characteristics of the TN mode, the four-domain TN (4DTN) structures were proposed [2-5]. However, these methods inevitably required a high pre-tilt angle (about 20°) to obtain a stable 4DTN structure. Hence, the conventional 4DTN modes exhibit low transmittance and/or slow response compared to the one-domain TN modes [6]. Moreover, complicated alignment processes are involved to obtain the high pre-tilt angle, apart from the multi-alignment processes.

In this paper, we propose a novel method for fabricating a stable 4DTN structure with a conventional planar alignment layer for the TN modes. The stable 4DTN structure was fabricated by multiply rubbing the conventional planar alignment layer and injecting a nematic liquid crystal (NLC) in an isotropic phase under an applied electric field. In such situation, the 4DTN structures were electrically stabilized with cooling down to a nematic phase. Our electrically stabilized (ES) 4DTN exhibits the fast response equal to the TN mode and the high transmittance compared to the highly pre-tilted 4DTN modes.

2. Experiments

Figure 1 shows a schematic diagram of the cell configuration of our ES-4DTN structure. The planar alignment layer (Nissan chemical SE-7492) was spin-coated on the indium-tin-oxide (ITO) coated glass substrate, and the pre-baked at 100 °C for 10 min to evaporate solvent followed by hard-baking at 210 °C for 2 h for perfect imidization. The reverse rubbing processes were carried out with rubbing mask with 150 μm spacing. Two reverse-rubbed substrates were assembled perpendicular to each other to perform the 4DTN structure. The cell thickness was maintained using spacers of 4.3 μm. The NLC of MLC-6875 (E Merck) with positive dielectric anisotropy ($\Delta\varepsilon$ = 7.8) was injected into the assembled cell by capillary action in the isotropic phase with applying an external voltage of 20 V. After injection of the NLC, the cell was cooled down to room temperature under the applied voltage.

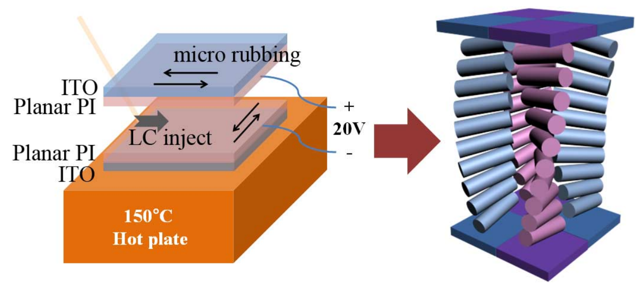

Figure 1. The schematic diagram of our ES-4DTN structure.

Measurements of the electro-optic (EO) transmittance and the dynamic EO response were carried out with a digitized oscilloscope (Tektronix TDS754D), an arbitrary waveform generator (Stanford Research System DS345), and a He-Ne laser (λ = 632.8 nm). The microscopic textures were observed with a charge-coupled devices (Samsung SDC-450) mounted in a polarizing microscope (Nikon Eclipse E600 POL). The micro-furnace (Mettler FP 90) was used for temperature control.

3. Results and Discussion

Figure 2 shows microscopic textures of our ES-4DTN structures. In the TN configuration, as you expect, no dark state is observed with rotating the sample cell under crossed polarizers. From Figs. 2(a) and 2(b), all domains exhibit the twisted configurations. Also, we checked the oppositely twisted directions between the adjacent domains like a chessboard by rotating the analyzer with respect to the polarizer as shown in Figs. 2(c) and 2(d). Since the chessboard pattern was inverted by converting the analyzer angle with respect to the polarizer from –45° to + 45°, two adjacent domains exhibit the oppositely twisted senses and thus the stable 4DTN structures were obtained by the electrical stabilization even in the planar alignment layer with a low pre-tilt angle.

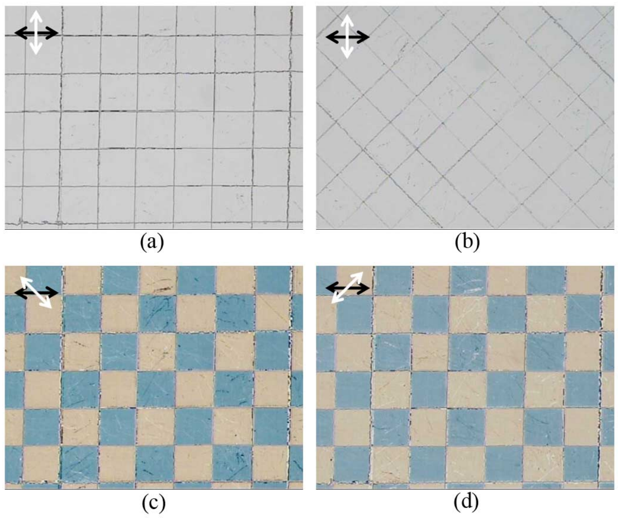

Figure 2. Optical microscope textures of our ES-4DTN cell at the various polarizer configurations. The rubbing directions are (a) parallel/perpendicular to one of the crossed polarizers and (b) rotated by 45°. The analyzers are rotated by (c) –45° and +45° from the polarizer compared to Fig. (a).

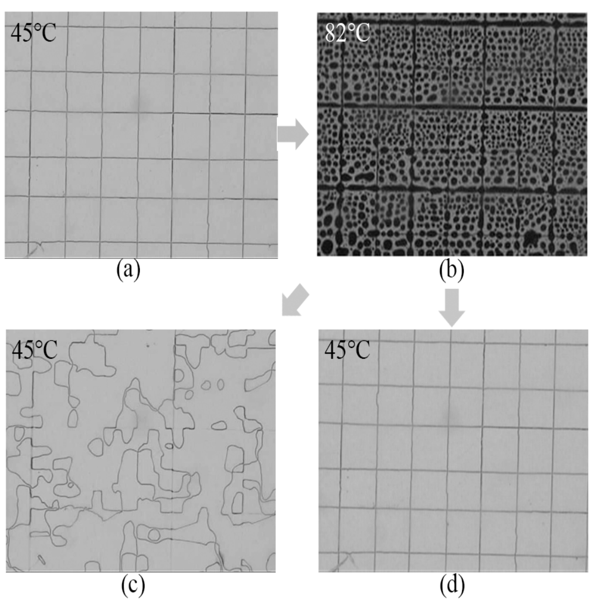

Figure 3. Optical microscopic textures of the 4DTN structures (a) cooled down under an applied voltage, (b) heated up near isotropic-nematic transition temperature, (c) cooled down again without the applied voltage, and (d) cooled down with the applied voltage. All textures were obtained under crossed polarizers in the absence of the applied voltage.

Figure 3 shows an electrical stabilization process of the 4DTN structures. The pre-tilt angle produced by rubbing the planar alignment layer is about 4° which is generally too low to stabilize the 4DTN structures in the absence of an applied voltage. Appying an external voltage in an isotropic phase and cooling down to a nematic phase under the applied voltage, the stable 4DTN structures were obtained even in the absence of the applied voltage as shown in Fig. 3(a). To investigate the electrical stabilization of the 4DTN structures, the sample cell was heated up to the isotropic-nemtic transition temperature as shown in Fig. 3(b). When the cell was cooled down to the nematic phase with no applied voltage, the 4DTN structures was eliminated at 0 V as shown in Fig. 3(c). When the cell was cooled down from the isotropic to the nematic phase with the applied voltage (20 V), the 4DTN structures was recovered as shown in Fig. 3(d). As a result, the stable 4DTN structures were obtained even through the pre-tilt angle of the alignment layer is lower than that required in a conventional 4DTN configuration

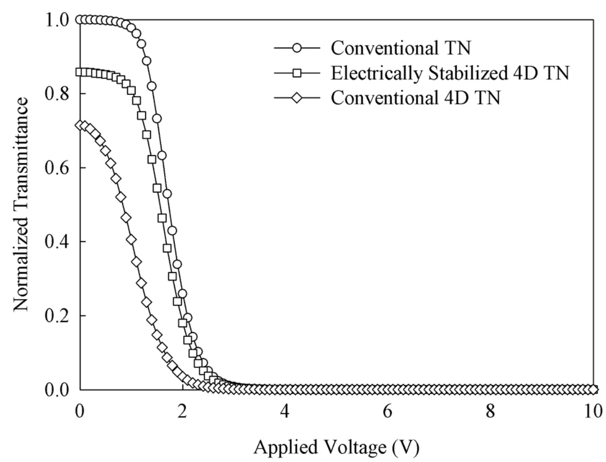

Figure 4. EO transmittances of the conventional 1DTN cell, the ES-4DTN cell, and the conventional 4DTN cell with high pre-tilt angle.

Figure 4 shows the EO transmittances of three different TN configurations: a conventional one-domain TN (1DTN), a conventional 4DTN with a high pre-tilt angle, and an ES-4DTN proposed here. The conventional 1DTN and the ES-4DTN were prepared with rubbing the planar alignment layer of SE-7492. The conventional 4DTN with a high pre-tilt angle was fabricated by stacking the planar and vertical alignments to produce a high pre-tilt angle (about 20°) [7]. Here, the pre-tilt angle is controlled by the thickness of the upper vertical alignment layer [8]. The thickness of the vertical alignment layer is governed by the spinning rate and the dilution percentage of solvent for the vertical alignment layer. In both 1DTN and the ES-4DTN cells, the same threshold behaviors were observed due to the same surface conditions such as the pre-tilt angle. On the other hand, the conventional 4DTN cell with the high pre-tilt angle exhibits a thresholdless behavior in the EO transmittance due to the high pre-tilt angle. The maximum transmittances of both 4DTN cells are lower than that of the 1DTN due to the disclination lines in the 4DTN structures.

In general, the cell thickness in the TN mode is determined by the first maximum condition of $\Delta n_{eff} d / \lambda = \sqrt{3}/2$ to obtain the fast response. The effective birefringence Δn_{eff} in the conventional 4DTN cell is smaller than that in the ES-4DTN cell due to the high pre-tilt angle. Therefore, the transmittance of the conventional 4DTN cell is reduced for the same cell thickness condition as shown in Fig. 4. When the cell thickness was optimized to obtain the same maximum transmittance as the ES-4DTN, the response time would be degraded.

Figure 5 shows the relaxation time characteristics of three different TN configurations. The dynamic behavior in the ES-4DTN mode coincides with that in the 1DTN mode except for the microscopic hydrodynamics near the disclination lines due to the same surface condition such as the pre-tilt angle and the anchoring energy. Therefore, the response time characteristics in both 1DTN and ES-4DTN cells almost agree well with each other. In the conventional 4DTN with the high pre-tilt angle, however, the relaxation time is increased due to the small restoring force originated from the small elastic deformation and the small surface anchoring strength.

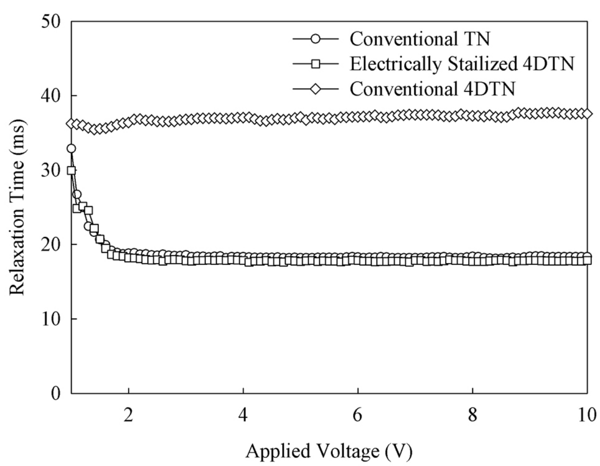

Figure 5. Relaxation time characteristics of the conventional 1DTN cell, the ES-4DTN cell, and the conventional 4DTN cell with high pre-tilt angle.

Figure 6 shows the long-term stability of our ES-4DTN cell at 0 V. From the microscopic images of the ES-4DTN cell at various times elapsed after forming the 4DTN structure at 0 V, we confirm that the ES-4DTN structure is stable even in the planar alignment layer with a low pre-tilt angle.

4. Conclusion

We proposed the stable 4DTN structure fabricated with the electrical stabilization using the cooling process from the isotropic phase to the nematic one under an applied voltage on the conventional planar alignment layer with a low pre-tilt angle. The ES-4DTN structure was fabricated by multiply rubbing the conventional planar alignment layer and injecting a nematic liquid crystal (NLC) in an isotropic phase under an applied electric field. In our ES-4DTN mode, the fast response equal to the TN mode and the high transmittance compared to the highly pre-tilted 4DTN modes were obtained.

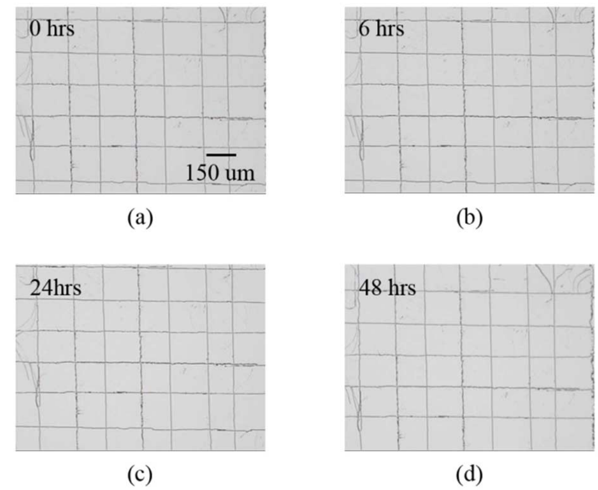

Figure 6. Microscopic images of our ES-4DTN under crossed polarizers at (a) 0, (b) 6, (c) 24, and (d) 48 h after the cell fabrication.

5. Acknowledgement

This research was supported by a grant (F0004121-2010-32) from Information Display R&D Center, one of the Knowledge Economy Frontier R&D Program funded by the Ministry of Knowledge Economy of Korean government and Samsung Electronics, Co. Ltd.

References

[1] A. Lien, H. Takano, S. Suzuki, and H. Uchida, Mol. Cryst. Liq. Cryst. **198**, 37 (1991).

[2] Y. Yamagnchi, T. Miyashita, and T. Uchida, J. Soc. Inf. Disp. 1993. 277.

[3] Y. Koike, T. Kamada, and M. Okabe, SID1992 Digest (1992) p. 798.

[4] S. Varghes, G. P. Crawford, C. W. M. Bastiaansen, D. K. G. De Boer, and D. J. Broer, Appl. Phys. Lett. **85**, 230 (2004).

[5] J. Chen. P. J. Bos, D. L. Johnson, D. R, Bryant, J. Li, S. H. Jamal, and J. R. Kelly, J. Appl. Phys. **80**, 1985 (1996).

[6] M. Reichenstein, H. Stark, J. Stelzer, and H.-R. Trebin, Phys. Rev. E **65**, 011709 (2001).

[7] Y.-K. Moon, S. I. Jo, K.-S. Bae, Y.-J. Lee, C.-J. Yu, and J.-H. Kim, SID2010 Digest (2010) p. 1748.

[8] Y.-J. Lee, J. S. Gwag, Y.-K. Kim, S. I. Jo, S.-G. Kang, Y. R. Park, and J.-H. Kim, Appl. Phys. Lett. **94**, 041113 (2009).